Opti-Morph, a new platform for sandy beach dynamics by constrained wave energy minimization

Megan Cook, Frédéric Bouchette, Bijan Mohammadi, Samuel Meulé, Nicolas Fraysse

Opti-Morph, a new platform for sandy beach dynamics by constrained wave energy minimization

Ronan Dupont[1,2,3*], Megan Cook[1,2,3†], Frédéric Bouchette[1,3†], Bijan Mohammadi[2,3†] and Samuel Meulé[1,3†]

[1*]GEOSCIENCES-M, Univ Montpellier, CNRS, Montpellier, France.
[2]IMAG, Univ Montpellier, CNRS, Montpellier, France.
[3]GLADYS, Univ Montpellier, Le Grau-du-Roi, France.

*Corresponding author(s). E-mail(s): ronan.dupont@umontpellier.fr;
Contributing authors: megan.cook@umontpellier.fr; frederic.bouchette@umontpellier.fr; bijan.mohammadi@umontpellier.fr; meule@cerege.fr;
†These authors contributed equally to this work.

Abstract

This paper focuses on a new approach to describe coastal morphodynamics, based on optimization theory, and more specifically on the assumption that a sandy seabed evolves in order to minimize a wave-related function, the choice of which depends on what is considered the driving force behind the coastal morphodynamic processes considered. The numerical model derived from this theory uses a gradient descent method and allows us to account for physical constraints such as sand conservation in basin experiments. Hence, the model automatically adapts to either basin or open sea settings and only involves two hyper-parameters: sand abrasion and the critical angle of repose. The Opti-Morph model is illustrated on a flume configuration. Comparison of the resulting seabed with experimental data as well as the results of the widely distributed coastal morphodynamic software XBeach demonstrates the potential of a model by wave energy minimization.

Keywords: Hydro-morphodynamics, Optimization, Model validation, Coastal, Variational approach, Energy minimization, Optimal transport, Waves.

1 Introduction

Optimization theory is the study of the evolution of a system while searching systematically for the minimum of a function derived from physical properties of the system. In this paper, we have applied this approach to coastal dynamics, with our primary objective to simulate the interactions between the waves and seabed. Using mathematical optimization theory [1–9], we have designed a model that describes the evolution of the seabed while taking into account the coupling between morphodynamic and hydrodynamic processes. This study focuses on a theoretical and numerical approach to the modeling of this coupling, based on the assumption that the seabed adapts to minimize a certain wave-related function. The choice of this function determines the driving force behind the morphological evolution of the seabed. This optimization problem is subjected to a certain number of constraints, allowing for a more accurate description of the morphodynamic evolution.

This study is accompanied by the development of a numerical hydro-morphodynamic model, which has the advantages of being fast, robust, and of low complexity. The model was given the name *Opti-Morph*.

The paper starts with a description of the simple hydrodynamic model used to calculate the driving forces behind the morphodynamic processes. Then, we provide a description of the morphodynamic model (Opti-Morph) based on wave-energy minimization. With the purpose of validating Opti-Morph, we compare the results of the numerical simulation with that of experimental data acquired in a flume experiment. We also compared the model to another nearshore hydro-morphodynamic model, XBeach [10], to see how it fares against existing hydro-morphodynamic models, XBeach being considered to be quite a reputable model in the coastal dynamic community [11–13].

1.1 State of the Art

Numerical models of morphodynamic processes are seen as a valuable tool for understanding and predicting the evolution of the sediment and morphology over time in coastal areas. Different morphodynamic models exist in the literature, ranging from empirical models [14–17] to process-based models. The latter can be sorted into several categories, such as i) profile evolution models [18–20], which use only cross-shore transport, ii) 2D morphological models [10, 21–29], which use depth-averaged wave and current equations to model the sediment transport while neglecting the vertical variations of wave-derived parameters, as well as iii) 3D and quasi-3D models [30–36], which determine

the sediment evolution using both horizontal and vertical variations of the wave-derived parameters.

The Opti-Morph model described in this paper is based on optimal control. In the past, the use of optimization theory has primarily been used in the design of coastal defense structures, whether in the design of ports and offshore breakwaters [2, 3].

Optimal control has already been considered for the modeling of shallow water morphodynamics, based on the assumption that the seabed acts as a flexible structure and adapts to a certain hydrodynamic quantity [4, 8]. These studies were based on somewhat theoretical developments with no direct relationship with real case studies. Our objectives in this work is to produce a physically robust numerical morphodynamic model based on optimal control and to validate it using numerical data from well established morphodynamics software and also basin experiments.

1.2 Hypotheses

Opti-Morph is based on a certain number of assumptions. Since the model is based on the minimization of a cost function, certain hypotheses must be made regarding the choice of this function. This function, which originates from a physical quantity, must be directly linked to the elevation of the seabed. At present, we set the quantity to be minimized as the energy of shoaling waves. This implies that the seabed reacts to the state of the waves by minimizing the energy of shoaling waves. Other assumptions assess the behavior of seabed and originate from general observations. Sediment transport is influenced by the orbital velocity of water particles [37], which leads to greater sediment mobility in shallower waters. Another natural observation concerns the slope of the seabed, which cannot be overly steep without an avalanching process occurring [38]. Last, in an experimental flume configuration, the quantity of sand must remain constant over time, with no inflow or outflow of sand to alter the sand stock.

2 Theoretical Developments

2.1 Modeling Framework

For the sake of simplicity, we present the principle of morphodynamics by optimization in a one-dimensional setting. This enables us to compare the numerical results based on this theory with experimental flume data. However, no assumptions were made regarding the dimension of the problem, and as a result, it is straightforward to extend this theory to a two-dimensional configuration.

We consider a coordinate system composed of a horizontal axis x and a vertical axis z. We denote $\Omega := [0, x_{\max}]$ the domain of the cross-shore profile of the active coastal zone, where $x = 0$ is a fixed point in deep water where no significant change in bottom elevation can occur, and $x_{\max}$ is an arbitrary point

at the shore beyond the shoreline, as shown by Figure 1. The elevation of the seabed is a one-dimensional positive function, defined by: $\psi : \Omega \times [0, T] \times \Psi \rightarrow \mathbb{R}^+$ where $[0, T]$ is the duration of the simulation (s) and Ψ is the set of physical parameters describing the characteristics of the seabed. In order to model the evolution over time of ψ and given the assumption that the seabed ψ changes over time in response to the energy of shoaling waves, a description of the surface waves is needed.

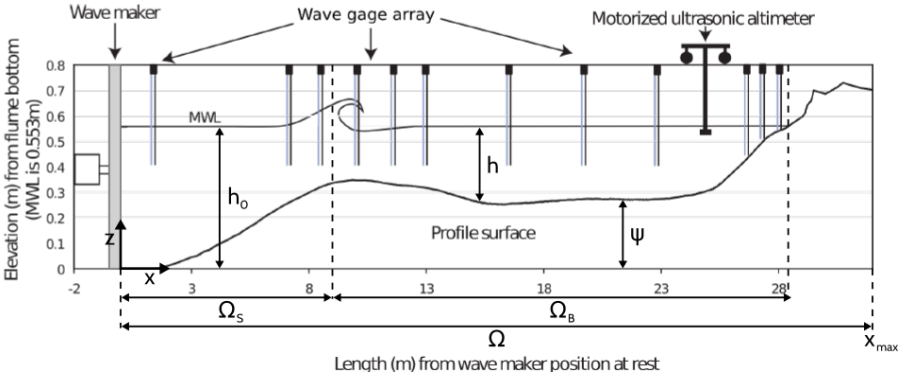

Fig. 1 Diagram of a cross-shore profile in the case of an experimental flume.

2.2 Hydrodynamic Model

The literature on hydrodynamic models is vast [39]. However, our main focus in this work is a) on the morphodynamic part of the approach and b) on providing evidence of the ability of optimization to perform robust morphodynamic prediction even under weakly constrained hydrodynamics. So we present the procedures with a hydrodynamic model as simple as possible, that is based on the linear wave theory [40], a very basic shoaling equation and some geometrical breaking parameter. It has the advantage of being easy to differentiate compared to more sophisticated models that would need automatic differentiation [6, 41] or huge additional numerical developments. This numerical implementation has a significantly short run-time as shown by the convergence results of the section 4.1. This model has the advantage of expressing wave height as an explicit function of the seabed, which leads to rapid calculations of the morphodynamic model.

Let h be the depth of the water from a mean water level h_0 (cf. Figure 1). Ocean waves, here assumed monochromatic, are characterized by phase velocity C, group velocity C_g, and wave number k, determined by the linear dispersion relation (1), where σ is the pulsation of the waves and g is the gravitational acceleration.

$$\sigma^2 = gk \tanh(kh) \tag{1}$$

We define Ω_S as the time-dependent subset of Ω over which the waves shoal and Ω_B the subset of Ω over which the waves break, cf. Figure 1. Munk's breaking criterion [42] enables us to define $\Omega_S(t) = \left\{x \in \Omega, \frac{H(x,t)}{h(x,t)} < \gamma\right\}$ and $\Omega_B(t) = \left\{x \in \Omega, \frac{H(x,t)}{h(x,t)} \geq \gamma\right\}$, where γ is a wave breaking index.

Then we have

$$H(x,t) = H_0(t)K_S(x,t) \tag{2}$$

The height of the waves H over the cross-shore profile is inspired by the shoaling equation (2), where $H_0(t)$ is the deep water wave height and K_S is a shoaling coefficient, given by

$$K_S = \left(\frac{1}{2}\frac{C_0}{C_g}\right)^{\frac{1}{2}} \tag{3}$$

where C_0 is the deep water wave velocity, and:

$$n = \frac{C}{C_g}, \quad C = C_0 \tanh(kh), \quad C_g = \frac{1}{2}C\left(1 + \frac{2kh}{\sinh(2kh)}\right). \tag{4}$$

Instead of considering that waves depend solely on offshore wave height H_0, this model suggests that shoaling waves are decreasingly influenced by seawards waves. The greater the distance, the less effect it has on the present wave height. As such, we introduce a weighting function w. Assuming that the maximal distance of local spatial dependency of a wave is denoted d_w, the weighting function over the maximal distance d_w is given by $w : [0, d_w] \to \mathbb{R}^+$ such that $w(0) = 1$, $w(d_w) = 0$ and decreases exponentially.

Equation (2) for shoaling wave height becomes equation (5), where H_0^w is defined by (6).

$$H(x,t) = H_0^w(x,t)K_S(x,t) \tag{5}$$

$$H_0^w(x,t) = \frac{1}{\int_{x-X}^{x} w(x-y)\mathrm{d}y}\int_{x-X}^{x} w(x-y)H(y)K(y)\mathrm{d}y \tag{6}$$

Equation (5) applies only to the shoaling, nearshore-dependent waves of Ω_S, significant wave height over the cross-shore profile $H : \Omega \to \mathbb{R}^+$ is defined by (7), where $\alpha(x) = \dfrac{x}{d_w}$ over $[0, d_w]$ to allow a smooth transition between offshore and nearshore-dependent waves.

$$H(x,t) = \begin{cases} \left[(1-\alpha(x))H_0(t) + \alpha(x)H_0^w(x,t)\right]K_S(x,t) & \text{if } x \in \Omega_S \text{ and } x < d_w \\ H_0^w(x,t)K_S(x,t) & \text{if } x \in \Omega_S \text{ and } x \geq d_w \\ \gamma h(x,t) & \text{if } x \in \Omega_B \end{cases} \tag{7}$$

2.3 Morphodynamic Model by Wave Energy Minimization

The evolution of the seabed is assumed to be driven by the minimization of a cost function J. Recalling the hypotheses made in Section 1.2 , the shape of the seabed is determined by the minimization of the potential energy of shoaling waves, for all $t \in [0, T]$:

$$J(\psi, t) = \frac{1}{16} \int_{\Omega_S} \rho_w g H^2(\psi, x, t) \mathrm{d}x \qquad [J.m^{-1}] \tag{8}$$

where H denotes the height of the waves over the cross-shore profile, ρ_w is water density ($kg.m^{-3}$), and g is the gravitational acceleration ($m.s^{-2}$). In order to describe the evolution of the seabed, whose initial state is given by ψ_0, we assume that the seabed ψ, in its effort to minimize J, verifies the following dynamics:

$$\begin{cases} \psi_t = \Upsilon \ \Lambda \ d \\ \psi(t=0) = \psi_0 \end{cases} \tag{9}$$

where ψ_t is the evolution of the seabed over time $[m.s^{-1}]$, Υ is the abrasion of sand ($m.s.kg^{-1}$), Λ is the excitation of the seabed by the water waves, and d is the direction of the descent, which indicates the manner in which the seabed changes. The approach involves two parameters with clear physical interpretation. The first Υ takes into account the physical characteristics of the sand and represents the mobility of the sediment. At the present time, we consider Υ to be a measure of sand mobility expressed in $m.s.kg^{-1}$. Further explanation of the nature of this parameter will be given at a later stage of the model's development. The second parameter Λ is a local function which represents the influence of the water depth on the seabed and is defined using the term describing the vertical variation of the classic velocity potential of the linear wave theory [37]:

$$\begin{aligned} \varphi : \Omega \times [0, h_0] &\longrightarrow \mathbb{R}^+ \\ (x, z) &\longmapsto \frac{\cosh(k(x)(h(x) - (h_0 - z)))}{\cosh(k(x)h(x))} \end{aligned} \tag{10}$$

In unconstrained circumstances, for instance, if a total sand volume constraint does not need to be enforced, we set $d = -\nabla_\psi J$, which indicates a direction for local minimization of J with regards to ψ. The calculation of $\nabla_\psi J$ is described in Appendix A.1. However, constraints are added to the model to incorporate more physics and deliver more realistic results. Driving forces behind the morphological evolution of the seabed are described by the minimization of the cost function J. Secondary processes are expressed by constraints. In the interest of simplicity, we have adopted two physical constraints though more can be introduced if necessary. The first concerns the slope of the seabed. Depending on the composition of the sediment, the slope of the

seabed is bounded by a grain-dependent threshold M_{slope}[40]. This is conveyed by the following constraint on the local bathymetric slope:

$$\left|\frac{\partial \psi}{\partial x}\right| \leq M_{\text{slope}} \tag{11}$$

The dimensionless parameter M_{slope} represents the critical angle of repose of the sediment, and varies between 0.2 and 0.6 [43].

A second example concerns the sandstock in the case of an experimental flume. This constraint states that the quantity of sand in a flume must be constant over time, as given by (12), contrarily to an open-sea simulation where sand can be transported between the onshore and the offshore zones [44, 45].

$$\int_{\Omega} \psi(t,x)\mathrm{d}x = \int_{\Omega} \psi_0(x)\mathrm{d}x \qquad \forall t \in [0,T] \tag{12}$$

This constraint is necessary for verifying and validating the numerical model with physical simulations.

3 Numerical Application

In this section, we present the numerical results produced by the Opti-Morph model. For validation purposes, the resulting seabed is compared to experimental data acquired during a flume tank experiment. We also conduct a comparative analysis between the physical seabed, the seabed produced by Opti-Morph and the seabed produced by XBeach, with the aim of assessing how Opti-Morph holds up against existing hydro-morphodynamic models. A brief description of the experiment is provided, as well the XBeach model.

3.1 Description of the Experiment

The experimental observations have been collected as part of the COPTER project and a series of laboratory wave-flume experiments were performed in order to investigate the morphodynamic impact of introducing solid geotextile tubes to the Hatzuk (Israel) seafloor [46]. We use the data collected without tubes to describe the natural evolution of the seabed over time.

A glass flume measuring 36 m long, 0.55 m wide and 1.3 m deep is equipped with a wave-maker and gauges measuring the height of the water. Artificial particles are placed inside the flume representing the mobile sea bottom and an ultrasonic gauge is used to measure the sedimentary topography.

The experimental seabed, described in Figure 1 is subjected to a series of 30-minute storm climates, among which a typical moderate storm event (at the scale of the flume) with a significant wave height and period of $H_{\text{s}} = 135\,mm$ and $T_{\text{s}} = 2.5\,s$. Time and length scale ratio are set to 1/3 and 1/10 respectively to that of the field.

3.2 XBeach Model

XBeach is an open-source process-based model developed by Deltares, UNESCO-IHE, and Delft University of Technology to simulate the hydro-morphodynamic processes in coastal areas [10–13].

In brief, XBeach uses four interconnected modules to model near-shore processes [47]. The two hydrodynamic modules consist of the short wave module and the flow module. The first is based on wave action equations [48], and incorporates breaking, dissipation [49], and wave current interactions, while the latter is governed by shallow water equations [50, 51]. One of the two morphodynamic modules is the sediment transport module based on the equilibrium sediment concentration equation [52] and a depth-averaged advection-diffusion equation [53]. The other is the morphology module which concerns seabed transformations such as the evolution of the seabed and avalanching.

In order to configure the XBeach model for the experimental flume setting, we refer to the XBeach user manual [54]. The domain Ω is defined over 32 m with a uniform subdivision of 320 cells. The incoming wave boundary condition is provided using a JONSWAP wave spectrum [55], with a significant wave height of $H_{\mathrm{m0}} = 0.015\,m$ and a peak frequency at $f_{\mathrm{p}} = 0.4s^{-1}$. The breaker model uses the Roelvink formulation [49], with a breaker coefficient of $\gamma = 0.4$, a power $n = 15$, and a wave dissipation coefficient of 0.5. These parameters were calibrated using the hydrodynamic data produced during the physical flume experiment. Concerning sediment parameters, the $D50$ coefficient is set as 0.0006, and the porosity is $2650\,kg.m^{-3}$. No other parameters such as bed friction or vegetation were applied. The model is set to run for a period of $1800\,s$, as a short-term simulation.

3.3 Hydrodynamic Validation

This section is devoted to the comparison of the two numerical hydrodynamic models to the experimental wave data obtained in the experimental flume of Section 3.1. Mean wave height profiles were calculated over the short-term storm simulation, for both Opti-Morph and XBeach, and compared to the mean wave height of the experimental model. The latter was calculated using the measures taken by the gauges of the flume.

Figure 2 shows that the hydrodynamic module of both Opti-Morph (red) and XBeach (blue) are both comparable with respect to the experimental measurements (green) excluding, as is often the case, the second point at $x = 6\,m$. XBeach demonstrates a close qualitative fit over the 10-22 m section of the flume, whereas Opti-Morph excels at the coast (21-27 m), with a near-perfect fit with the experimental data. Despite the simplicity of the hydrodynamic model used by Opti-Morph, the resulting wave height is of the same order of magnitude over the cross-shore profile than that measured during the flume experiment, which indicates that the resulting seabeds are comparable with regard to the forcing energy driving the morphodynamic response.

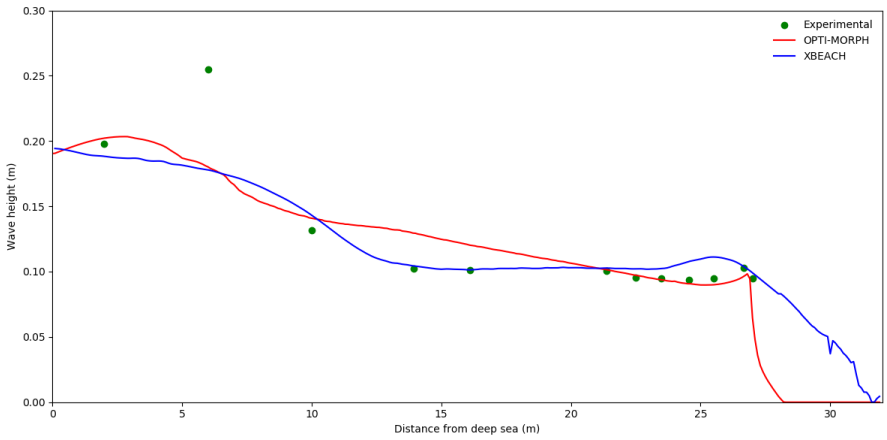

Fig. 2 Comparison of mean wave height over a storm simulation. The green points correspond to the mean wave height provided by the gauges of the flume experiment. The mean wave height determined by Opti-Morph (red) and XBeach (blue) also appears. The non-zero wave height beyond the shoreline as presented by XBeach is due to wave set-up, which Opti-Morph does not handle.

3.4 Numerical Results of the Morphodynamic Simulations

The Opti-Morph model was applied to the configuration of the COPTER experiment of Section 3.1, and the resulting beach profile is shown by the red profile, in Figure 3.A. The main observation is the decrease of $2.5\,cm$ in height of the sandbar, at $x = 9\,m$. We observe a slight decrease of the seabed adjacent to the wave-maker, and a slight increase at the plateau, situated at 15-25 m. No mobility is observed at the coast.

When comparing the results provided by Opti-Morph (red), with that of XBeach (blue) and the experimental data (green), as shown on Figure 3.A, we observe that the red seabed profile provided by the Opti-Morph model shows a general quantitative agreement when compared to the experimental data, as does the XBeach morphological module. In fact, both models produce profiles close to the experimental data over the plateau located at 15-25 m from the wave-maker (Fig. 3.C). At the shore, Opti-Morph matches the experimental data whereas XBeach shows a vertically difference of up to $3\,cm$ at $x = 27\,m$ (Fig. 3.D). Discrepancies on the part of both models occur in the area surrounding the tip of the sandbar, as both Opti-Morph and XBeach fail to predict the shoreward shift of the sandbar (Fig. 3.B); the experimental data show that the height of the sandbar remains unchanged with regards to the initial profile. Both sandbars have a height of $0.375\,m$; however, the sandbar resulting from the experimental simulation has moved towards the coast, an occurrence that neither numerical model was able to predict.

As such, this new model based on wave-energy minimization shows potential when compared to XBeach, in the case of short-term simulations.

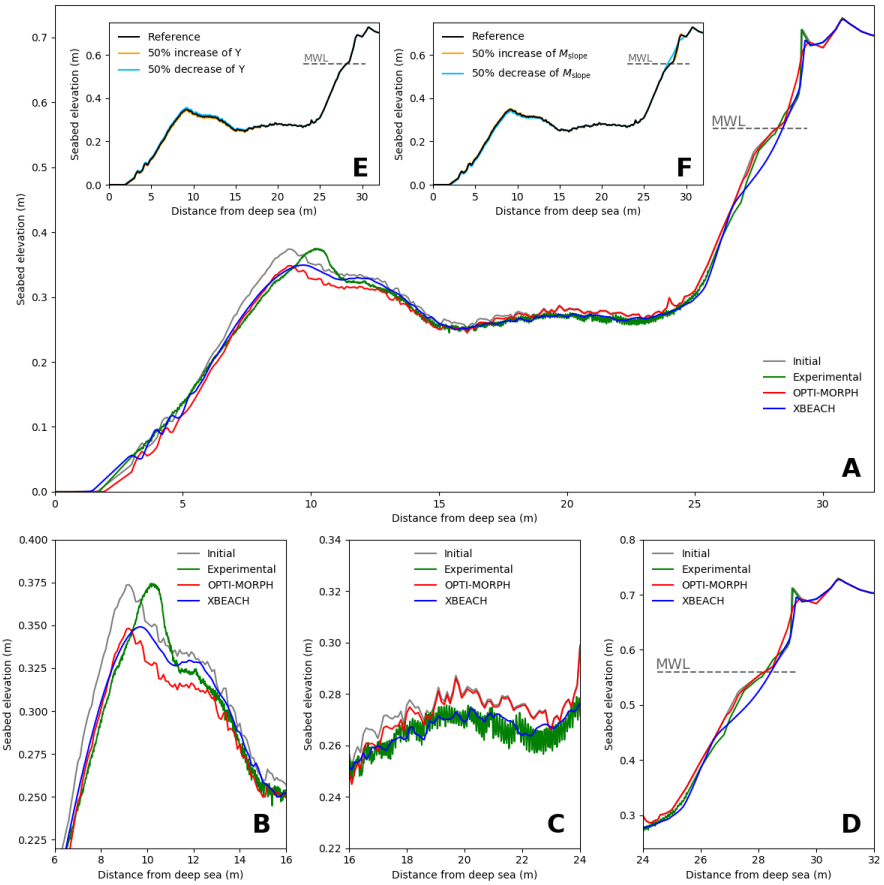

Fig. 3 **A.** Results of the numerical simulation calculated over the initial seabed (gray) using the XBeach morphodynamic module (blue) and the Opti-Morph model (red). These are compared with the experimental data acquired during the COPTER project (green). The mean water level is denoted MWL and is set at $0.56\,m$. **B.** Zoomed in view of the sandbar, located between $6\,m$ and $16\,m$. **C.** Zoomed in view of the plateau, located between $16\,m$ and $24\,m$. **D.** Zoomed in view at the shoreline, located between $24\,m$ and $32\,m$. **E.** Robustness analysis of the mobility parameter Υ. The reference profile is depicted in black. The orange (resp. light blue) profile is the result of a 50% increase (resp. decrease) in mobility, with all other parameters remaining the same. **F.** Robustness analysis of the maximal sand slope parameter M_{slope}. The reference profile is depicted in black. The orange (resp. light blue) profile is the result of a 50% increase (resp. decrease) of M_{slope} , with all other parameters remaining the same.

4 Discussion

4.1 Robustness analysis of the convergence in time and space of the hydrodynamic model

We computed a reference OPTIMORPH simulation using a very small time step of $0.05\,s$ which is much smaller than what is usually used in hydro-morphodynamic simulations. The simulation was performed with the original bathymetric profile of the COPTER experiment and the forcings of the wave maker.

This simulation provides a reference computed sea bed $\psi_{ref}(t_f, x)$ at some given time t_f.We would like to see the convergence toward this reference solution of various other OPTIMORPH simulations with different decreasing time steps. From this series of simulations, we quantify a residual error with L^2 norm as $\mathcal{E}_{L^2} = ||\psi_{ref} - \psi||_{L^2}$ in [m]. We performed 10 simulations with time steps ranging in $[0.05;\ 160]\,s$ and we get the results described in figure 4.a).

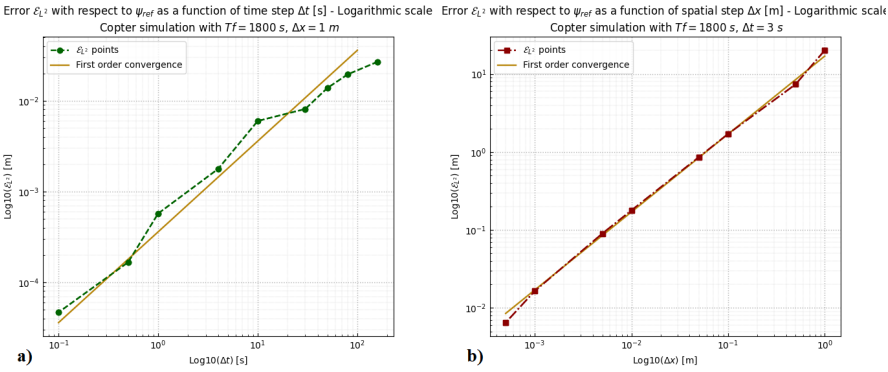

Fig. 4 a) Errors $\mathcal{E}_{L^2}$ (green) obtained by simulations of 10 different time steps compared to the reference simulation corresponding to a time step of $0.05\,s$. First order convergence (yellow). b)l Errors $\mathcal{E}_{L^2}$ (red) obtained by simulations of 10 different spatial steps compared to the reference simulation corresponding to a spatial step of $0.0002\,m$. First order convergence (yellow).

In order to analyze the convergences in space and time, we choose, respectively, a reference time step of $\Delta t = 3\,s$ and a spatial step size $\Delta x = 1\,m$. $\Delta t = 3\,s$ corresponds to the kind of time steps we would like to use in simulations. But, we will use larger spatial resolution in practice. The results in figure 4 show first order (illustrated by the continuous line) convergence rates in both time and space.

To understand why a time step of 3 seconds is interesting for computing efficiency, it is useful to look at the CFL stability condition analysis for the shallow-water Saint-Venant model. The analysis provides a typical upper

bound for the time step of the form:

$$\Delta t = \min_i \left(\frac{\Delta x}{2 \max_i (|u_i \pm \sqrt{g h_i}|)} \right) = \frac{\Delta x}{2 \max_i (|u_0 \pm \sqrt{g h_0}|)},$$

where subscript i indicates the mesh node which means that the minimum is taken over all the nodes of the mesh. In our situation, it correspond to the off-shore position (subscript $i = 0$). Typicals values in our simulation are: $u_0 = 10\, m.s^{-1}$, $\Delta x = 1\, m$, $h = 0.55\, m$ and $g = 9.81\, m.s^{-2}$. This gives us $\Delta t = 0.04\, s$, which is about two orders of magnitude smaller than our reference time step of $\Delta t = 3\, s$. In addition, the costs of one iteration of the Saint-Venant and Optimorph models are comparable.

4.2 Parameter Robustness Analysis

One of the advantages of the Opti-Morph model is the low number of morphodynamic hyper-parameters required. At the present time, Opti-Morph requires two hyper-parameters: the mobility parameter Υ and the maximal slope parameter M_{slope}. Here, an assessment on these parameters is conducted. In Figure 3.E, three simulations were performed in identical settings with changes made solely to the mobility parameter. Initially, this parameter Υ has a value of 5×10^{-6}, $m.s.kg^{-1}$. Figure 3.E shows no significant difference despite a 50% increase ($\Upsilon = 7.5 \times 10^{-6}\, m.s.kg^{-1}$) (orange) or decrease ($\Upsilon = 2.5 \times 10^{-6}\, m.s.kg^{-1}$) (light blue) of Υ with regard to the baseline seabed profile (black). Similar conclusion can be deduced for the maximal slope parameter M_{slope}, whose reference value here is 0.2. The corresponding parameter of XBeach is *wetslp*, described in the XBeach manual as the critical avalanching slope under water, and is also set to 0.2. In Figure 3.F, we observe little difference between the reference seabed (black), the seabed resulting from a 50% increase ($M_{\text{slope}} = 0.3$) (orange) and the seabed resulting from a 50% decrease ($M_{\text{slope}} = 0.1$) (light blue). The only apparent discrepancy can be found at $x = 28\, m$, where the seabed is at its steepest, and therefore the sand slope constraint is more prone to be active. The reduction of the critical angle of repose results naturally in a less steep slope. The robustness of Opti-Morph in relation to both the mobility parameter and the slope parameter, despite a significant increase or decrease of their value, is apparent. Further simulations show that the robustness of these parameters is not specific to this particular flume configuration, but can be observed regardless of the initial configuration.

4.3 Long-term Simulations

This section is devoted to the long-term behavior of Opti-Morph, the main question being, is this numerical model capable of creating an equilibrium state after being subjected to a great number of repeated events. Five forcing scenarios, lasting either 2 or 6 days, were applied to the same initial seabed in the same parametric configuration. The current Opti-Morph code is in Python.

Typically, using time-steps of $1\,s$ simulating a day of forcing requires about 1.5 hours on a 2GHz PC computer. Each time iteration gathering the steps presented in this paper requires therefore about $63\,ms$. Regarding the section 4.1, we could use $3\,s$ time-step and divide the simulation time by 3. An analysis of the resulting seabeds is performed as well as their behavior throughout the simulation. The latter is achieved through a comparative study of four time-series, focusing on: (1), the vertical evolution of seabed elevation at the tip of the sandbar; (2), the vertical evolution of seabed elevation at a point of the plateau; (3), the distance between the wave-maker and the onset of the seabed; and (4), the location of the shoreline position.

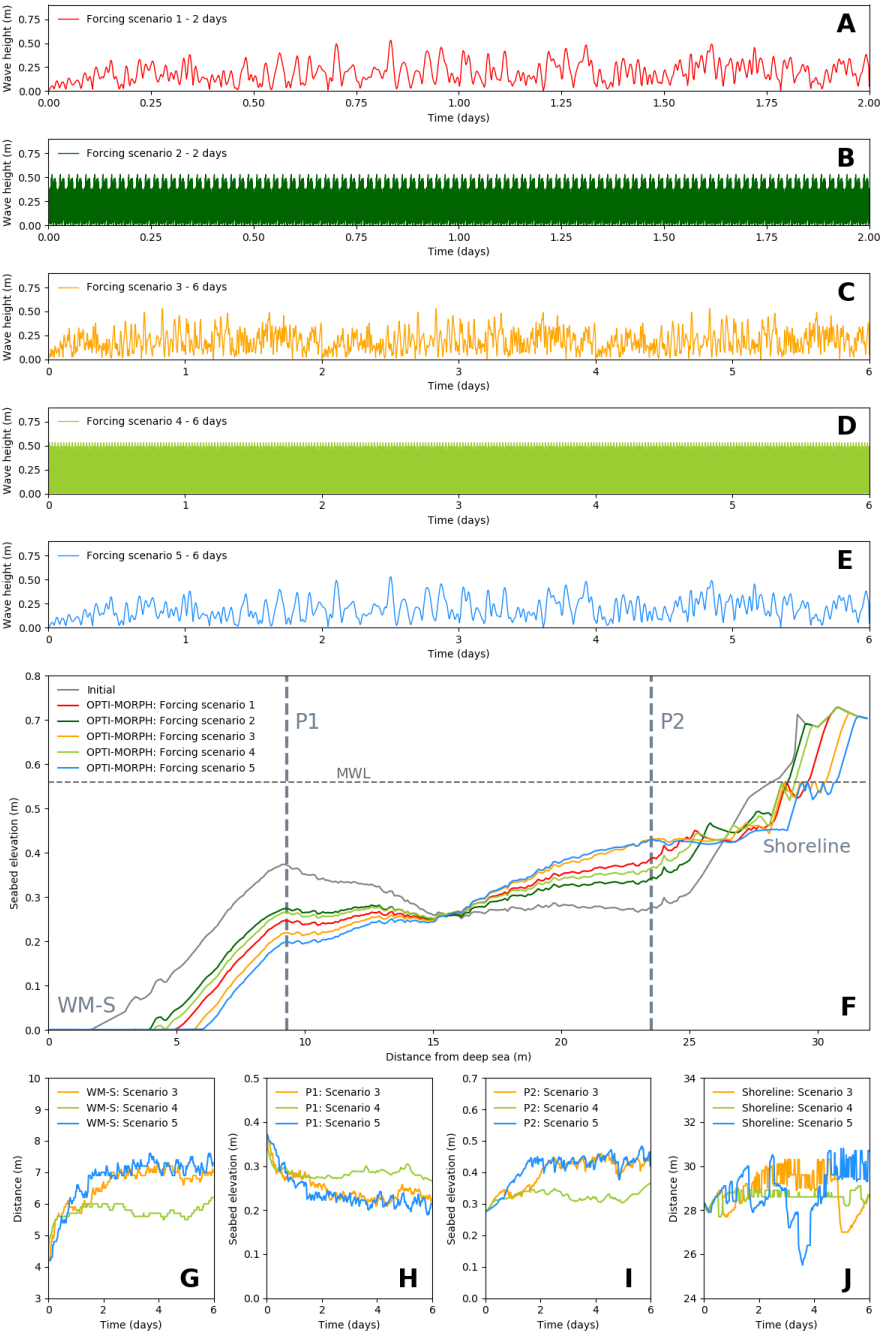
Forcing scenario 1 - 2 days
A
Forcing scenario 2 - 2 days
B
Forcing scenario 3 - 6 days
C
Forcing scenario 4 - 6 days
D
Forcing scenario 5 - 6 days
E
Wave height (m)
Time (days)
Initial
OPTI-MORPH: Forcing scenario 1
OPTI-MORPH: Forcing scenario 2
OPTI-MORPH: Forcing scenario 3
OPTI-MORPH: Forcing scenario 4
OPTI-MORPH: Forcing scenario 5
P1
P2
MWL
Shoreline
WM-S
F
Seabed elevation (m)
Distance from deep sea (m)
WM-S: Scenario 3
WM-S: Scenario 4
WM-S: Scenario 5
G
P1: Scenario 3
P1: Scenario 4
P1: Scenario 5
H
P2: Scenario 3
P2: Scenario 4
P2: Scenario 5
I
Shoreline: Scenario 3
Shoreline: Scenario 4
Shoreline: Scenario 5
J
Distance (m)

Fig. 5 Long-term simulation of Opti-Morph. **A.** Forcing wave height for scenario 1, composed of several long-term events over a 2-day period. **B.** Forcing wave height for scenario 2, composed of numerous short-term events over a 2-day period. **C.** Forcing wave height for scenario 3, composed of several long-term events over a 6-day period. **D.** Forcing wave height for scenario 4, composed of numerous short-term events over a 6-day period. **E.** Forcing wave height for scenario 5, composed of few long-term events over a 6-day period. **F.** Seabeds resulting from the different forcing scenarios produced by Opti-Morph. Two points of interest have be identified: P1 located at $x = 9.3\,m$ and P2 located at $x = 20.1\,m$. **G.** Evolution of the distance, devoid of sediment, between the wave-maker (located at $x = 0\,m$) and the seabed (WM-S), regarding forcing scenarios 3, 4, and 5. **H.** Vertical evolution of seabed elevation at P1, driven by the 6-day forcing scenarios 3, 4, and 5. **I.** Vertical evolution of seabed elevation at P2, driven by the 6-day forcing scenarios 3, 4, and 5. **J.** Evolution of shoreline position, driven by the 6-day forcing scenarios 3, 4, and 5.

Applying Opti-Morph over a longer time-series leads to the results of Figure 5. The two 2-day forcing scenarios are shown in Figures 5.A and 5.B. In both cases, we observe that the resulting seabeds of Figure 5.F are subjected to the destruction of the sandbar and have a tendency to evolve progressively towards an equilibrium beach profile [56]. Simulations over a 6-day period were conducted to confirm this tendency. These scenarios are depicted in Figures 5.C, 5.D, and 5.E, and the resulting seabeds given in Figure 5.F show once again the destruction of the sandbars, the elevation of the plateau, and erosion at the shoreline. Furthermore, all three tend towards an equilibrium state. This is confirmed by the four time-series analysis presented in Figures 5.G, 5.H, 5.I, and 5.J. The vertical elevation of the seabed at both points P1 and P2 show initial variations over the first 2 days: a decrease in the case of P1 (cf. Figure 5.H) and an increase in the case of P2 (cf. Figure 5.I). However, both studies show a stabilization of the seabed elevation over the last 4 days of the 6-day period. Similar conclusions can be drawn regarding the length of the zone containing no sediment adjacent to the wave-maker (cf. Figure 5.G). An initial increase between 2 and 3 meters can be observed, with stability achieved in the later stages of the simulations. Finally, Figure 5.J shows the evolution of the shoreline position. Initially found at $x = 28.3\,m$, all scenarios provoke a retreat of the shoreline: $0.4\,m$ in scenario 3, $0.3\,m$ in scenario 4, and $2\,m$ in scenario 5. The shorelines of the latter two converge, whereas scenario 3 shows an abrupt advance of the shoreline at day 5, with an attempt to return back to its stable state of $x = 30\,m$. The seabed has been flattened, the sandbar has been destroyed and erosion can be observed at the coast [57]. This tendency to evolve towards an equilibrium state [40] is consistent with the choice of morphogenic and constant storm-like forcing conditions.

The comparisons made between the two 2-day simulations and the three 6-day simulations, in this given configuration, also reveal the little influence heritage has on the morphodynamic response. Both scenarios 1 and 2 have a comparable cumulative incoming wave energy density $E = \frac{1}{16}\int_0^T \rho g H_0^2 \mathrm{d}t$ of $0.0591\,J.m^{-2}$. The resulting seabeds evolve towards similar profiles (reduction of the sandbar, increase of elevation of the plateau, and erosion at the coast), despite two different forcing conditions. Similar conclusions can be

drawn regarding the 6-day simulations, where the cumulative energy density of all three is equal to $0.177\,J.m^{-2}$.

5 Conclusions

Opti-Morph shows potential as a fast, robust, and low complexity morphodynamic model involving only two hyper-parameters. Despite using a basic hydrodynamic model for the description of the complex coupling of hydrodynamic and morphodynamic processes, we can nevertheless observe that a numerical model based on an optimization theory works effectively, with comparable results to a state of the art hydro-morphodynamic model requiring the tuning of dozens of hyper-parameters. Long-term simulations also show typical morphodynamic behavior, with the tendency of the seabed to evolve towards an equilibrium state. These results demonstrate the tremendous potential of Opti-Morph, a constrained energy minimization morphodynamic model.

6 Declarations

6.1 Availability of data and material

All data, models, and code generated or used during the study appear in the submitted article.

6.2 Conflict of interest

The authors declare that they have no conflict of interest.

6.3 Acknowledgements

Appendix A Mathematical Developments

In this section, we detail some of the mathematical results needed in the implementation of the Opti-Morph model, specifically the calculation of the gradient of the cost function J (Eq. (8)) with regard to the bathymetry ψ, which in turn requires the gradient of the wave height function (Eq. (7)) with regard to ψ. With the current choice of hydrodynamic model, this can be achieved analytically. With more sophisticated hydrodynamic models this is not always possible. In these cases, if the source code of the model is available, the calculation of the gradient can be performed using automatic differentiation of programs [41, 58] directly providing a computer program for the gradient.

A.1 Gradient of the Cost Function with respect to the Bathymetry

Opti-Morph requires the evaluation of gradient of the functional J with respect to the bathymetry ψ, denoted $\nabla_\psi J$. For a general functional of the form $J(\psi(x), H(\psi(x)))$ involving dependencies with respect to the bathymetry and

hydrodynamic quantities H, this sensitivity can be expressed using the chain rule:

$$\nabla_\psi J = \partial_\psi J + \partial_H J \, \partial_\psi H \tag{A1}$$

where $\partial_\psi J = \frac{\partial J}{\partial \psi}$. $\partial_\psi H$ requires the linearization of the hydrodynamic model, and ψ is a parametric representation of the bathymetry.

A.2 Gradient of the Wave Height with respect to the Bathymetry

This section is devoted to the calculation of the gradient of the wave height H, given by (7), with regards to the seabed elevation ψ and denoted $\partial_\psi H$. Being as $h = h_0 - \psi$, the derivation of the third line of (7) with regards to ψ is immediate. The calculation of the gradient of the first line of (7) is analogous to that of the second. It remains to differentiate the second line of (7) with regards to ψ. Observing that the chain rule yields for all $x, t \in \Omega_S \times [0, T]$ with $x \geq d_w$,

$$\partial_\psi H(x,t) = H_0^w(x,t)\partial_\psi K_S(x,t) + \partial_\psi H_0^w(x,t) K_S(x,t), \tag{A2}$$

and that the term $\partial_\psi H_0^w(x,t)$ can be determined iteratively, using $\partial_\psi H_0 = 0$, it remains to determine $\partial_\psi K_S(x,t)$. Injecting the definitions of n, C and C_g, given in (4), yields

$$K_S = \left[\tanh(kh)\left(1 + \frac{2kh}{\sinh(2kh)}\right)\right]^{1/2}. \tag{A3}$$

For the sake of simplicity, let $U = \tanh(kh)\left(1 + \frac{2kh}{\sinh(2kh)}\right)$ and $X = kh$. Equation (A3) becomes

$$\partial_\psi K_S = -\frac{1}{2}\, U^{-3/2}\, \partial_\psi U, \tag{A4}$$

and we have

$$\partial_\psi U = \partial_\psi X \frac{2\cosh^2(X) - X\sinh(2X)}{\cosh^4(X)}, \tag{A5}$$

with $\partial_\psi X = h\partial_\psi k + k\partial_\psi h = h\partial_\psi k - k$. Moreover, differentiating both sides of the dispersion equation (1) by ψ gives

$$\partial_\psi k = \frac{k^2}{\cosh(kh)\sinh(kh) + kh}. \tag{A6}$$

Combining (A4),(A5), and (A6), we obtain $\partial_\psi K_S$, and therefore $\partial_\psi H$.

References

[1] Isèbe, D., Azérad, P., Bouchette, F., Mohammadi, B.: Design of passive defense structures in coastal engineering **5**(2), 75. https://doi.org/10.15866/irece.v5i2.2029. Accessed 2022-04-01

[2] Isebe, D., Azerad, P., Mohammadi, B., Bouchette, F.: Optimal shape design of defense structures for minimizing short wave impact. Coastal Engineering **55**(1), 35–46 (2008). https://doi.org/10.1016/j.coastaleng.2007.06.006

[3] Isèbe, D., Azerad, P., Bouchette, F., Ivorra, B., Mohammadi, B.: Shape optimization of geotextile tubes for sandy beach protection. International Journal for Numerical Methods in Engineering **74**(8), 1262–1277 (2008). https://doi.org/10.1002/nme.2209

[4] Bouharguane, A., Azerad, P., Bouchette, F., Marche, F., Mohammadi, B., ,Institut de Mathématiques et de Modélisation de Monptellier, Université Montpellier II, 34 095 Montpellier: Low complexity shape optimization & a posteriori high fidelity validation. Discrete & Continuous Dynamical Systems - B **13**(4), 759–772 (2010). https://doi.org/10.3934/dcdsb.2010.13.759. Accessed 2022-04-01

[5] Bouharguane, A., Mohammadi, B.: Minimization principles for the evolution of a soft sea bed interacting with a shallow. International Journal of Computational Fluid Dynamics **26**, 163–172 (2012). https://doi.org/10.1080/10618562.2012.669831

[6] Mohammadi, B., Bouharguane, A.: Optimal dynamics of soft shapes in shallow waters **40**(1), 291–298. https://doi.org/10.1016/j.compfluid.2010.09.031. Accessed 2022-03-11

[7] Mohammadi, B., Bouchette, F.: Extreme scenarios for the evolution of a soft bed interacting with a fluid using the value at risk of the bed characteristics. Computers and Fluids **89**, 78–87 (2014). https://doi.org/10.1016/j.compfluid.2013.10.021

[8] Mohammadi, B., Bouharguane, A.: Optimal dynamics of soft shapes in shallow waters. Computers and Fluids **40**, 291–298 (2011). https://doi.org/10.1016/j.compfluid.2010.09.031

[9] Cook, M., Bouchette, F., Mohammadi, B., Sprunck, L., Fraysse, N.: Optimal port design minimizing standing waves with a posteriori long term shoreline sustainability analysis **35**(6), 802–813. https://doi.org/10.1007/s13344-021-0071-7. Accessed 2022-04-01

[10] Roelvink, D.J.A., Reniers, A., van Dongeren, A., Thiel de Vries, J.,

McCall, R., Lescinski, J.: Modelling storm impacts on beaches, dunes and barrier islands. Coastal Engineering **56**, 1133–1152 (2009). https://doi.org/10.1016/j.coastaleng.2009.08.006

[11] Zimmermann, N., Trouw, K., Wang, L., Mathys, M., Delgado, R., Verwaest, T.: Longshore transport and sedimentation in a navigation channel at blankenberge (belgium). Coastal Engineering Proceedings **1** (2012). https://doi.org/10.9753/icce.v33.sediment.111

[12] Bugajny, N., Furmanczyk, K., Dudzinska-Nowak, J., Paplińska-Swerpel, B.: Modelling morphological changes of beach and dune induced by storm on the southern baltic coast using xbeach (case study: Dziwnow spit). Journal of Coastal Research **I**, 672–677 (2013). https://doi.org/10.2112/SI65-114.1

[13] Williams, J., Esteves, L., Rochford, L.: Modelling storm responses on a high-energy coastline with xbeach. Modeling Earth Systems and Environment **1** (2015). https://doi.org/10.1007/s40808-015-0003-8

[14] de Vriend, H., Bakker, W.T., Bilse, D.P.: A morphological behaviour model for the outer delta of mixed-energy tidal inlets. Coastal Engineering **23**, 305–327 (1994). https://doi.org/10.1016/0378-3839(94)90008-6

[15] Gravens, M.: An approach to modeling inlet and beach evolution, pp. 4477–4490 (1997). https://doi.org/10.1061/9780784402429.348

[16] Kana, T., Hayter, E.J., Work, P.: Mesoscale sediment transport at southeastern u.s. tidal inlets: conceptual model applicable to mixed energy settings. Journal of Coastal Research **15**, 303–313 (1999)

[17] Ruessink, G., Terwindt, J.H.J.: The behaviour of nearshore bars on the time scale of years: A conceptual model. Marine Geology **163**, 289–302 (2000). https://doi.org/10.1016/S0025-3227(99)00094-8

[18] Larson, M., Kraus, N.: Sbeach: Numerical model for simulating storm-induced beach change. report 1. empirical foundation and model development. Technical report, DEPARTMENT OF THE ARMY US Army Corps of Engineers, Washington, DC, USA (July 1989)

[19] Larson, M., Kraus, N., Byrnes, M.: Sbeach: Numerical model for simulating storm-induced beach change. report 2. numerical formulation and model tests. Technical report, DEPARTMENT OF THE ARMY US Army Corps of Engineers, Washington, DC, USA (May 1990)

[20] Nairn, R., Southgate, H.: Deterministic profile modelling of nearshore processes. part 2. sediment transport and beach profile development. Coastal Engineering **19**, 57–96 (1993). https://doi.org/10.1016/0378-3839(93)

90019-5

[21] Fleming, C., Hunt, J.: Application of sediment transport model, pp. 1184–1202 (1977). https://doi.org/10.1061/9780872620834.070

[22] Latteux, B.: Harbour design including sedimentological problems using mainly numerical technics, pp. 2213–2229 (1980). https://doi.org/10.1061/9780872622647.133

[23] Coeffe, Y., Pechon, P.: Modelling of sea-bed evolution under waves action. Proc. 18th ICCE **1** (1982). https://doi.org/10.9753/icce.v18.71

[24] Yamaguchi, M., Nishioka, Y.: Numerical simulation on the change of bottom topography by the presence of coastal structures, pp. 1732–1748 (1985). https://doi.org/10.1061/9780872624382.118

[25] Watanabe, A., Maruyama, K., Shimizu, T., Sakakiyama, T.: Numerical prediction model of three-dimensional beach deformation around a structure. Coastal Engineering Journal **29**, 179–194 (1986). https://doi.org/10.1080/05785634.1986.11924437

[26] Maruyama, K., Takagi, T.: A simulation system of near-shore sediment transport for the coupling of the sea-bottom topography, waves and currents. Proc. IAHR Symp. Math. Mod. Sed. Transp. Coastal Zone, 300–309 (1988)

[27] Wang, H., Miao, G., Lin, L.-H.: A time—dependent nearshore morphological response model, pp. 2513–2527 (1993). https://doi.org/10.1061/9780872629332.192

[28] Johnson, H., Brøker, I., Zyserman, J.: Identification of some relevant processes in coastal morphological modelling, pp. 2871–2885 (1995). https://doi.org/10.1061/9780784400890.208

[29] Nicholson, J., Brøker, I., Roelvink, D.J.A., Price, D., Tanguy, J.-M., Moreno, L.: Intercomparison of coastal area morphodynamic models. Coastal Engineering - COAST ENG **31**, 97–123 (1997). https://doi.org/10.1016/S0378-3839(96)00054-3

[30] Roelvink, J.A., Van Banning, G.K.F.M., Verwey, A.: Design and development of delft3d and application to coastal morphodynamics, 1st international conference, hydroinformatics 94. In: Hydroinformatics 94, HYDROINFORMATICS -PROCEEDINGS-, 1st International Conference, Hydroinformatics 94, vol. 1, pp. 451–456. Balkema, Rotterdam (1994)

[31] Lesser, G.R., Roelvink, D.J.A., Kester, J.A.T.M., Stelling, G.: Development and validation of a three-dimensional morphological model. Coastal Engineering **51**, 883–915 (2004). https://doi.org/10.1016/j.coastaleng.2004.07.014

[32] Roelvink, D.J.A., Walstra, D.-J., Chen, Z.: Morphological modelling of keta lagoon case, pp. 3223–3236 (1995). https://doi.org/10.1061/9780784400890.233

[33] Briand, M.-H., Kamphuis, J.W.: Sediment transport in the surf zone: A quasi 3-d numerical model. Coastal Engineering **20**, 135–156 (1993). https://doi.org/10.1016/0378-3839(93)90058-G

[34] Zyserman, J., Johnson, H.: Modelling morphological processes in the vicinity of shore-parallel breakwaters. Coastal Engineering **45**, 261–284 (2002). https://doi.org/10.1016/S0378-3839(02)00037-6

[35] Ding, Y., Wang, S., Jia, Y.: Development and validation of a quasi-three-dimensional coastal area morphological model. Journal of Waterway Port Coastal and Ocean Engineering **132**, 462–476 (2006). https://doi.org/10.1061/(ASCE)0733-950X(2006)132:6(462)

[36] Droenen, N., Deigaard, R.: Quasi-three-dimensional modelling of the morphology of longshore bars. Coastal Engineering **54**, 197–215 (2007). https://doi.org/10.1016/j.coastaleng.2006.08.011

[37] Soulsby, R.L.: Calculating bottom orbital velocity beneath waves. Coastal Engineering - COAST ENG **11**, 371–380 (1987). https://doi.org/10.1016/0378-3839(87)90034-2

[38] Reineck, H.-E., Singh, I.B.: Depositional Sedimentary Environments; with Reference to Terrigenous Clastics [by] H.-E. Reineck [and] I. B. Singh, p. 439. Springer, (1973)

[39] Murray, A.B.: Reducing model complexity for explanation and prediction. Geomorphology **90**(3), 178–191 (2007). https://doi.org/10.1016/j.geomorph.2006.10.020. Reduced-Complexity Geomorphological Modelling for River and Catchment Management

[40] Dean, R., Dalrymple, R.: Coastal processes with engineering applications. Coastal Processes with Engineering Applications, by Robert G. Dean and Robert A. Dalrymple, pp. 487. ISBN 0521602750. Cambridge, UK: Cambridge University Press, March 2004. (2004)

[41] Hascoet, L., Pascual, V.: Tapenade user's guide. In: INRIA Technical Report, pp. 1–31. INRIA, (2004)

[42] Munk, W.: The solitary wave theory and its application to surf problems. Annals of the New York Academy of Sciences **51**, 376–424 (1949). https://doi.org/10.1111/j.1749-6632.1949.tb27281.x

[43] Beakawi Al-Hashemi, H.M., Baghabra Al-Amoudi, O.S.: A review on the angle of repose of granular materials. Powder Technology **330**, 397–417 (2018). https://doi.org/10.1016/j.powtec.2018.02.003

[44] Hattori, M., Kawamata, R.: Onshore-Offshore Transport and Beach Profile Change, pp. 1175–1193 (1980). https://doi.org/10.1061/9780872622647.072

[45] Quick, M.: Onshore-offshore sediment transport on beaches. Coastal Engineering **15**, 313–332 (1991)

[46] Bouchette, F.: Coastal defense strategy along hatzuk beach (northern tel aviv, israel). insights from the copter physical experimentation with moveable bed. Technical Report 17-1, BRL Ingénierie, Nîmes (March 2017)

[47] Daly, C.: Low frequency waves in the shoaling and nearshore zone a validation of xbeach. Erasmus Mundus Master in Coastal and Marine Engineering and Management (CoMEM), Delft University of Technology (2009)

[48] Holthuijsen, L., Booij, N., Herbers, T.H.C.: "a prediction model for stationary, short crested waves in shallow water with ambient current". Coastal Engineering **13**, 23–54 (1989). https://doi.org/10.1016/0378-3839(89)90031-8

[49] Roelvink, D.J.A.: Dissipation in random wave groups incident on a beach. Coastal Engineering - COAST ENG **19**, 127–150 (1993). https://doi.org/10.1016/0378-3839(93)90021-Y

[50] Andrews, D.G., Mcintyre, M.E.: An exact theory of nonlinear waves on a lagrangian-mean flow. Journal of Fluid Mechanics **89**(4), 609–646 (1978). https://doi.org/10.1017/S0022112078002773

[51] Walstra, D.-J., Roelvink, D.J.A., Groeneweg, J.: Calculation of wave-driven currents in a 3d mean flow model, vol. 276 (2000). https://doi.org/10.1061/40549(276)81

[52] Soulsby, R.: Dynamics of Marine Sands. Thomas Telford Publishing, (1997). https://doi.org/10.1680/doms.25844

[53] Galappatti, G., Vreugdenhil, C.: A depth-integrated model for suspended sediment transport. Journal of Hydraulic Research **23**(4), 359–377 (1985)

[54] Roelvink, D.J.A., Reniers, A., van Dongeren, A., Thiel de Vries, J., Lescinski, J., McCall, R.: Xbeach model – description and manual. Technical report, Unesco-IHE Institute for Water Education, Deltares and Delft University of Technology, Delft, Netherlands (January 2010)

[55] Hasselmann, K., Barnett, T.P., Bouws, E., Carlson, H., Cartwright, D., Enke, K., Ewing, J.A., Gienapp, H., Hasselmann, D., Kruseman, P., Meerburg, A., Muller, P., Olbers, D., Richren, K., Sell, W., Walden, H.: Measurements of wind-wave growth and swell decay during the joint north sea wave project (jonswap). Technical report, Deutsches Hydrographisches Institut, Hamburg, Germany (January 1973)

[56] of Engineers, U.A.C.: Coastal Engineering Manual, Engineer Manual 1110-2-1100. US Army Corps of Engineers, Washington, D.C. (2002)

[57] Grasso, F., Michallet, H., Barthélemy, E.: Experimental simulation of shoreface nourishments under storm events: A morphological, hydrodynamic, and sediment grain size analysis. Coastal Engineering **58**(2), 184–193 (2011). https://doi.org/10.1016/j.coastaleng.2010.09.007

[58] Griewank, A., Walther, A.: Evaluating Derivatives: Principles and Techniques of Algorithmic Differentiation, 2nd edn. Society for Industrial and Applied Mathematics, (2008). https://doi.org/10.1137/1.9780898717761